FEBS Letters 459 (1999) 218–222 FEBS 22640

The onset of atherosclerotic lesion formation in hypercholesterolemic rabbits is delayed by iron depletion

Durairaj Ponraj[a], Jagoda Makjanic[a], Patricia S.P. Thong[a], Benny K.H. Tan[b], Frank Watt[a,*]

[a] *Research Centre for Nuclear Microscopy, Department of Physics, National University of Singapore, Singapore 119260, Singapore*
[b] *Department of Pharmacology, National University of Singapore, Singapore, Singapore*

Received 21 July 1999; received in revised form 3 August 1999

Abstract The theory that iron may play a significant role in atherogenesis by promoting the formation of free radicals is controversial. Previous results using the new technique of nuclear microscopy showed a seven-fold increase in iron concentrations within newly formed atherosclerotic lesions in hypercholesterolemic rabbits compared to healthy artery tissue. In a follow-up time sequence study described here, we show that iron accumulation occurs at the onset of lesion formation. In addition, weekly bleeding decreases the iron uptake into the artery wall and delays the onset of atherogenesis. These results provide direct evidence for a key role of iron in initiating atherogenesis.

Key words: Iron; Atherosclerosis; Oxidative stress; Nuclear microscopy

1. Introduction

The substantial and growing evidence that oxidation of low density lipoproteins (LDLs) plays an important role in atherogenesis leads to the idea that 'catalytic' iron could also be involved by promoting the formation of free radical species. This idea was first proposed by Sullivan who noted the increased risk of coronary heart disease among men [1]. This theory has since found support in experimental studies showing the presence of 'catalytic' iron in advanced atherosclerotic lesions [2], together with epidemiological evidence showing a reduced risk of heart diseases among blood donors [3,4] and a link between dietary iron and heart disease [5,6]. Further support for the iron theory comes from observation of increased iron levels in both human and animal atherosclerotic lesions [7,8]. In the mouse model, an iron-deficient diet was shown to reduce atherosclerotic lesion formation [9]. Recent work has also shown that intralysosomal iron may contribute to the oxidation of LDLs, leading to cell damage induced by oxidized LDLs [10,11].

Nevertheless, the link between iron and atherosclerosis remains controversial. The search for epidemiological support for the association between iron status and heart diseases has thus far yielded both positive [3,4,12–14] and negative results [15–17]. In two experimental studies, iron overload increased oxidative stress in rats [18] and augmented the formation of atherosclerotic lesions in hypercholesterolemic rabbits [19], but in a similar study, iron overload was found to decrease rather than increase atherosclerosis in the rabbit model [20]. In humans, blood letting was shown to lower body iron stores and increase the oxidation resistance of serum lipoproteins [21]. However, iron overload of blood plasma did not lead to increased LDL oxidation in vitro [22].

In our previous work using the technique of nuclear microscopy, we have investigated changes in elemental concentrations in atherosclerotic lesions from hypercholesterolemic rabbit models. In this work we observed a seven-fold increase in iron within the lesion compared to healthy artery tissue [8], a result which is consistent with the hypothesis that iron may play a role in atherogenesis. However, the presence of iron does not mean that it plays a key role in the atherogenic process. In the present paper, we address this question directly by showing that iron depletion induced by weekly bleeding [21,23,24] not only reduces the iron accumulation in early lesions, but also delays the onset of atherogenesis.

2. Materials and methods

2.1. Rabbits

A total of 27 male hybrid (local × New Zealand White) rabbits with a mean weight of 2.5 kg were divided into three groups:

1. Normal group: three animals on a standard rabbit chow diet;
2. Cholesterol-fed group: 12 animals on a 1% cholesterol diet were killed after 4, 8, 12 or 16 weeks in groups of three. One 8-week animal reacted poorly to the diet and was not used in the analysis;
3. Bled cholesterol-fed group: 12 animals on a 1% cholesterol diet were subjected to weekly bleeding (15 ml/week) and killed after 4, 8, 12 or 16 weeks in groups of three. One 16-week animal did not survive and was not used in the analysis.

2.1.1. Rabbit feed Specially prepared no meat meal pellets containing 1% by weight cholesterol were supplied by Glen Forrest Stockfeeders (Glen Forrest, Western Australia).

2.2. Blood analysis

In order to check that all the cholesterol-fed animals were hypercholesterolemic, blood samples were taken at 0, 4, 8, and 12 weeks and subjected to standard lipid analysis including serum cholesterol levels (Department of Laboratory Medicine, National University Hospital, Singapore).

2.3. Sample preparation for nuclear microscopy

After each rabbit was killed, the aortic arch was removed and flash-frozen in liquid nitrogen. Sections of 10 μm were cut using a cryotome and freeze-dried on pioloform-coated target holders prior to nuclear microscopy studies. Pioloform (Agar Scientific) is a submicrometer polymer film used for supporting thin tissue sections in nuclear microscopy investigations.

2.4. Hematoxylin and eosin (H&E) staining

Sections from the same regions were also prepared for hematoxylin and eosin (H&E) staining as follows. The sections were rinsed in two changes of deionized water followed by Harris hematoxylin solution for 10 min. After this the sections were washed in two changes of deionized water, followed by a change in differentiating fluid. The sections were then washed in deionized water, tap water, deionized water followed by 3% eosin for 2–3 min. The sections were then

*Corresponding author. Fax: (65) 777 6126.
E-mail: phywattf@nus.edu.sg

PII: S0014-5793(99)01199-0

washed in three changes of absolute alcohol, followed by three changes of xylene and finally mounted in Permount and air-dried.

The H&E stained sections were not used in the nuclear microscope studies due to the potential risk of contamination and elemental redistribution during the staining process.

2.5. Nuclear microscopy

Two artery sections per animal were scanned using the National University of Singapore (NUS) nuclear microscope [25]. Three complementary ion beam techniques were carried out simultaneously using a 2 MeV proton beam focused to a 1 μm spot size. (1) Particle induced X-ray emission (PIXE) provided quantitative concentration measurements for elements with atomic numbers 11 (sodium) and above in the periodic table. X-rays were detected using a lithium-drifted silicon X-ray detector placed at 45° to the beam axis and fitted with a filter designed for optimal detection of trace elements such as iron in biological specimens [26]. (2) Rutherford backscattering spectrometry (RBS) provided information on matrix composition and incident charge dose, necessary to extract quantitative results in conjunction with PIXE. (3) Off-axis scanning transmission ion microscopy (STIM) provided information on the structure and density distribution of the section, and facilitated positioning of the unstained sections prior to analysis. (A more detailed description of nuclear microscopy can be found in [27].)

The nuclear microscope data acquisition software allows information to be extracted from user-defined regions of the scanned areas. Elemental concentrations were extracted from the entire artery wall cross-section, except for the region that includes the outer artery wall adjacent to fibrous tissue. This region was avoided during data analysis since it is especially prone to retaining blood.

2.6. Lesion imaging

Morphometric analysis of the H&E stained sections was carried out using a Zeiss light microscope interfaced to the Zeiss KS400 image analyzer software. The atherosclerotic lesion areas were mapped manually in three sections of the aortic arch per animal and expressed as square millimeters. The mean lesion areas were used as indicators of the extent of lesion development for that group and time interval.

2.7. Statistics and data presentation

All data in bar charts are presented as mean ± S.E.M. Two-tailed unpaired *t*-tests were performed to test for significance of difference between cholesterol-fed and bled cholesterol-fed data. In these data P values < 0.05 are indicated by * while P values < 0.01 are indicated by **.

3. Results

3.1. Blood analysis

Fig. 1 shows the mean serum cholesterol concentrations (mmol/l) in cholesterol-fed and bled cholesterol-fed animals at 0, 4, 8, and 12 weeks. The results confirm that all the animals in both groups were hypercholesterolemic.

3.2. Image analysis

Fig. 2a shows the mean lesion areas (mm^2) observed in H&E stained sections from cholesterol-fed and bled cholesterol-fed animals killed after 4, 8, 12 or 16 weeks. Fig. 2b shows an enlargement of the 4 and 8 week data. While the mean lesion areas in both groups increased over time, the lesion areas in bled cholesterol-fed animals were smaller compared to those in cholesterol-fed animals at each time interval.

3.2.1. Cholesterol-fed group. Fatty streaks were observed in the inner artery wall as early as 4 weeks and lesions were well developed by 8 weeks. By 12 and 16 weeks, these lesions had increased to occupy most of the artery walls.

3.2.2. Bled cholesterol-fed group. Little or no lesion formation was observed at 4 and 8 weeks. At 12 weeks, lesions were developing rapidly but there was still a significant difference in the lesion areas between the bled cholesterol-fed and the cholesterol-fed groups. At 16 weeks, the lesions were well developed.

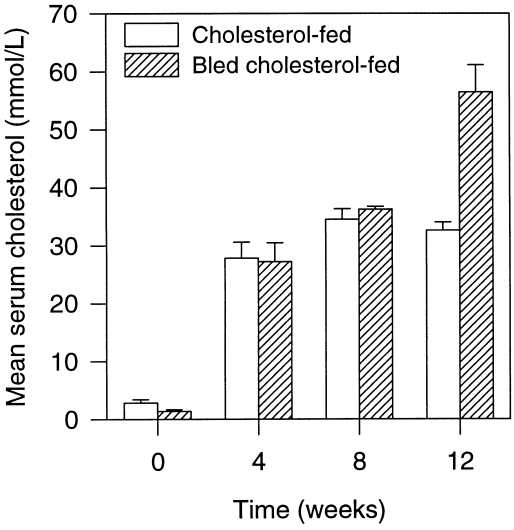

Fig. 1. Mean serum cholesterol concentrations (mmol/l) in surviving cholesterol-fed and bled cholesterol-fed animals at 0, 4, 8, and 12 weeks. Data are presented as mean ± S.E.M.

3.3. Correlation of stained sections with nuclear microscopic images

Fig. 3 shows the following representative images: (top row) H&E sections; (2nd row) off-axis STIM images of the unstained tissue sections; (3rd row) calcium distribution maps; and (bottom row) iron distribution maps. The columns are represented as follows: column 1 (normal); column 2 (8 week cholesterol-fed); column 3 (8 week bled cholesterol-fed); column 4 (16 week cholesterol-fed) and column 5 (16 week bled cholesterol-fed animals). The arrowheads within the H&E images indicate the inner walls of the arteries (or atherosclerotic lesions).

3.3.1. H&E sections. The beginning of an early lesion is apparent in the 8 week cholesterol-fed animal, but not in the 8 week bled cholesterol-fed animal. In the 16 week cholesterol-fed animal, the lesion is well developed and occupies well over 50% of the artery wall. The lesion in the bled cholesterol-fed animal is also well developed but is less extensive.

3.3.2. STIM images. These images indicate the density of

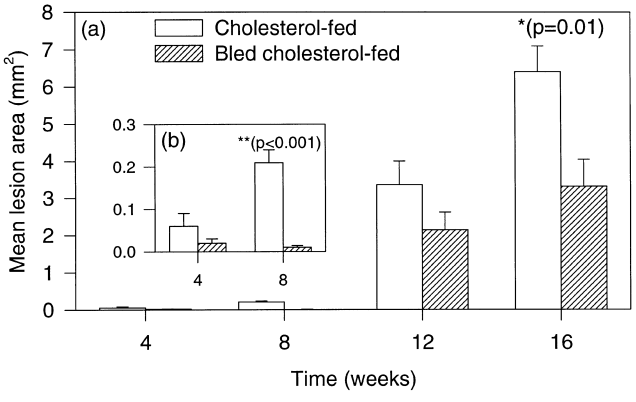

Fig. 2. Mean lesion areas (mm^2) observed in H&E stained sections from cholesterol-fed and bled cholesterol-fed animals killed at 4, 8, 12 or 16 weeks. Data are presented as mean ± S.E.M.

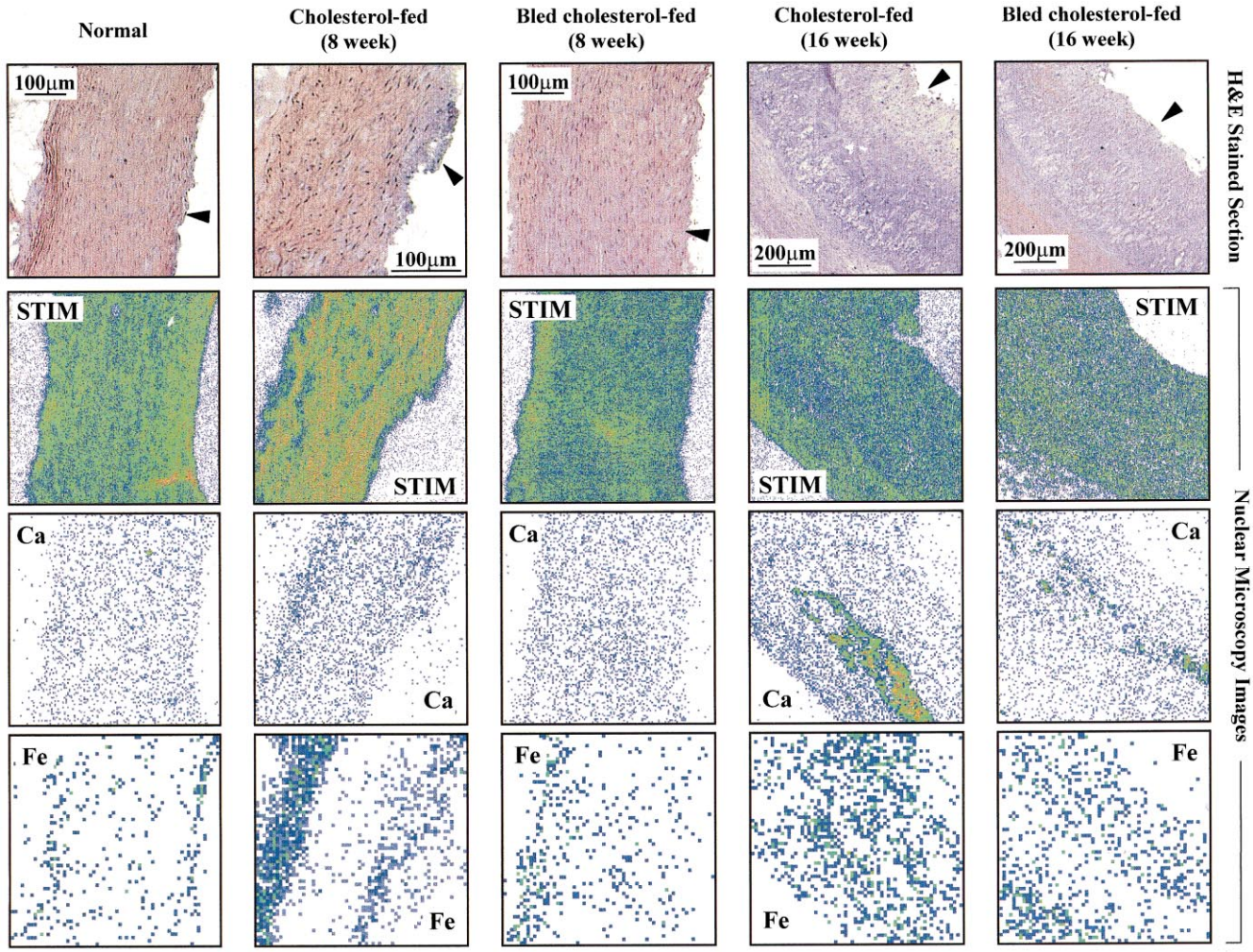

Fig. 3. The H&E stained section image (top row) and the off-axis STIM (2nd row), Ca and Fe distribution maps (3rd and bottom rows) from a normal (column 1), an 8 week cholesterol-fed (column 2), an 8 week bled cholesterol-fed (column 3), a 16 week cholesterol-fed (column 4) and a 16 week bled cholesterol-fed (column 5) animal. The arrowheads within the H&E images indicate the inner walls of the arteries.

the tissue, and act as a template for the Ca and Fe elemental maps.

3.3.3. Calcium maps. Calcium is observed to be at normal levels until the 16th week, at which time calcium granules are observed at the interface region between the lesion and the normal artery wall. The calcification process is more advanced in the 16 week cholesterol-fed animal compared with the 16 week bled cholesterol-fed animal.

3.3.4. Iron maps. High Fe levels on the outer wall in several of the sections are due to residual blood trapped by fibrous tissue adjacent to the artery. These regions were excluded from the elemental analyses (which are summarized in Fig. 4). There is an accumulation of Fe within the lesion in the 8 week cholesterol-fed animal. In contrast, the section from the 8 week bled cholesterol-fed animal indicates no increase in Fe at the inner wall. This is consistent with image analysis results showing little or no lesion in 8 week bled cholesterol-fed animals. High iron concentrations are observed to be widespread in the section from the 16 week cholesterol-fed animal, corresponding to the extended area occupied by the developed lesion. In the section from the 16 week bled cholesterol-fed animal, the iron concentration is lower and corresponds to the area occupied by the less developed lesion.

3.4. Quantitative results from nuclear microscopy

3.4.1. Elemental concentration data. The trends reflected in the representative elemental maps (Fig. 3) can be seen more quantitatively in Fig. 4, which shows the mean elemental concentrations (parts per million dry weight, ppm) of magnesium, phosphorus, sulfur, potassium, calcium, iron, copper, and zinc in the normal, cholesterol-fed and bled cholesterol-fed groups. The solid line in each bar chart shows the mean elemental concentration in normal animals, the dotted lines the S.E.M. Significant *t*-test probabilities for differences between concentrations in cholesterol-fed and bled cholesterol-fed animals are shown in parentheses. The following points can be noted:

- In the bled cholesterol-fed group, Mg, P, S, K, Ca, Fe and Zn concentrations remained close to normal levels at 4 and 8 weeks.
- At 4 weeks, Fe concentrations in the cholesterol-fed group (44 ppm) are significantly increased above those in normal (24 ppm) and bled cholesterol-fed (21 ppm) groups.
- At 8 and 12 weeks, a further increase in Fe to 69 ppm in the cholesterol-fed group was observed, while in the bled cho-

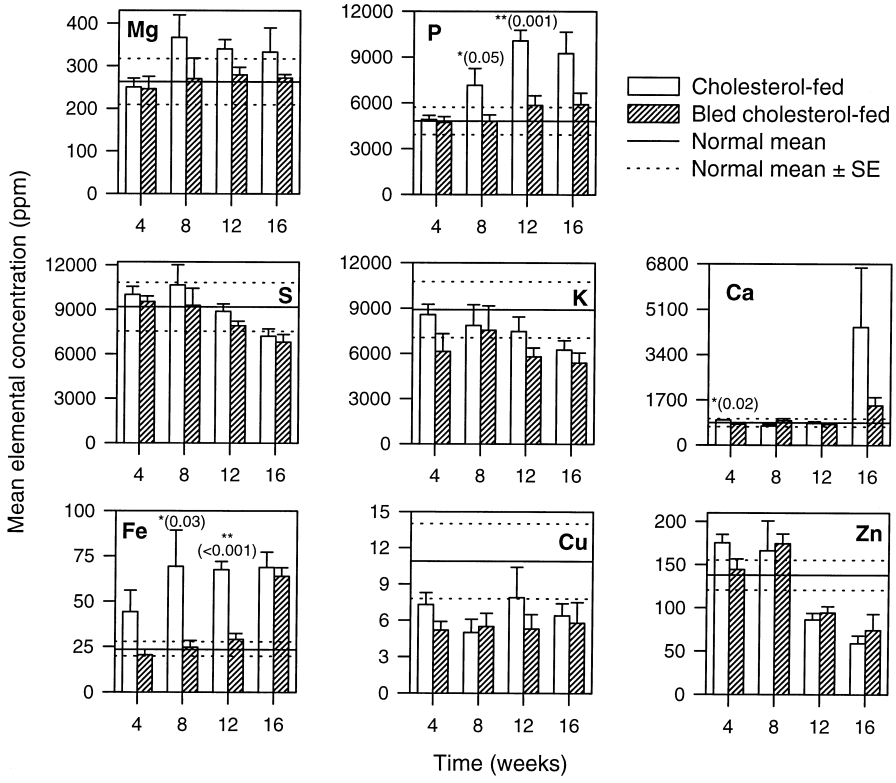

Fig. 4. Mean elemental concentrations (ppm) of Mg, P, S, K, Ca, Fe, Cu and Zn in artery wall sections taken from normal, cholesterol-fed and bled cholesterol-fed groups. Data are presented as mean ± S.E.M. The solid line in each bar chart shows the mean elemental concentration in normal animals, the dotted lines the S.E.M. The *P* values for significant differences between cholesterol-fed and bled cholesterol-fed concentrations are shown in parentheses.

lesterol-fed group the Fe concentration was close to normal levels.

- At 16 weeks, both the cholesterol-fed and bled cholesterol-fed groups showed higher levels of Fe (64 ppm) compared to normal animals.
- The P concentrations in cholesterol-fed animals increased above those in normal and bled cholesterol-fed animals at 8 weeks (7153 ppm), peaked at 12 weeks (10 078 ppm) and remained high at 16 weeks (9251 ppm).
- The sudden increase in Ca levels in cholesterol-fed animals (4433 ppm) and bled cholesterol-fed animals (1489 ppm) at 16 weeks is due to the appearance of granules rich in Ca and P at the interface between the lesion and healthy tissue and is consistent with calcification of the lesions observed at this stage.
- Cu levels in both cholesterol-fed and bled cholesterol-fed animals are consistently lower than the levels observed in normal animals at 4, 8, 12 and 16 weeks.
- Zn concentrations in both cholesterol-fed and bled cholesterol-fed animals at 12 and 16 weeks are significantly ($P < 0.05$) below concentrations in normal animals.

4. Discussion

Fatty streak lesions in cholesterol-fed animals were observed as early as 4 weeks into the high cholesterol diet. This onset of atherogenesis is accompanied by a two-fold increase in Fe levels (44 ppm) in the artery walls of animals fed a 1% cholesterol diet, compared to 21 ppm in animals fed the same diet but subjected to weekly bleeding. By 8 weeks, the difference between the Fe levels in cholesterol-fed and bled cholesterol-fed animals increased to almost three-fold (69 ppm compared to 25 ppm) ($P < 0.05$). Although the lesion areas in the cholesterol-fed group continued to increase throughout the 16 weeks, there was no further increase in Fe concentrations from 8 weeks. In the bled cholesterol-fed animals there was little or no lesion formation observed even after 8 weeks and the Fe concentrations in the artery walls at 4 and 8 weeks remained close to that in normal animals (24 ppm). These observations imply that (1) iron accumulation is an early event occurring at the onset of atherosclerotic lesion formation, and (2) weekly bleeding both decreases the uptake of iron into the artery wall and delays the onset of atherosclerotic lesion formation in hypercholesterolemic animals.

Our results are consistent with those of Yuan et al. who proposed a role for intralysosomal iron in initiating the oxidation of LDLs and lesion formation [10]. Possible mechanisms for iron accumulation in artery walls could be erythrophagocytosis by migrating macrophages, as they are known to play key roles in atherosclerosis [28], or via the action of heme oxygenase (see review by Jacob [29]).

Similar to the Fe concentrations, the P concentrations in cholesterol-fed animals also increased during the 16 week investigation. However, while the increase in Fe appeared to be an early event, the increase in P occurred only after 8 weeks and therefore appears to be a secondary effect. Since an increase in P has also been observed in Parkinson's disease [30], in which oxidative stress has also been implicated, P increase could be a secondary hallmark of oxidative damage.

The concentrations of Cu in both cholesterol-fed and bled cholesterol-fed animals were found to be below that of normal animals throughout the 16 weeks, and could reflect the effect of a high cholesterol diet on Cu levels. This is of potential significance as copper has been reported to be more effective than iron in oxidizing LDLs [31].

It is noted, from this current study, that the protective effect of blood depletion could not be sustained past 12 weeks. However, in light of the potentially important role of iron and copper in initiating atherogenesis, future work will focus on the effects of metal chelating drugs on atherosclerotic lesion formation and reduction.

References

[1] Sullivan, J.L. (1981) Lancet 1, 1293–1294.
[2] Smith, C., Mitchinson, M.J., Aruoma, O.I. and Halliwell, B. (1992) Biochem. J. 286, 901–905.
[3] Tuomainen, T.P., Salonen, R., Nyyssonen, K. and Salonen, J.T. (1997) Br. Med. J. 314, 793–794.
[4] Meyers, D.G., Strickland, D., Maloley, P.A., Seburg, J.J., Wilson, J.E. and McManus, B.F. (1997) Heart 78, 188–193.
[5] Ascherio, A., Walter, C.W., Rimm, E.B., Giovannucci, E.L. and Stampfer, M.J. (1994) Circulation 89, 969–974.
[6] Klipstein-Grobusch, K., Grobbee, D.E., den Breeijen, J.H., Boeing, H., Hofman, A. and Witteman, J.C.M. (1999) Am. J. Epidemiol. 149, 421–428.
[7] Pinheiro, T., Pallon, J., Fernandes, R., Halpern, M.J., Homman, P. and Malmqvist, K. (1996) Cell. Mol. Biol. 42, 89–102.
[8] Thong, P.S.P., Selley, M. and Watt, F. (1996) Cell. Mol. Biol. 42, 103–110.
[9] Lee, T.-S., Shiao, M.-S., Pan, C.-C. and Chau, L.-Y. (1999) Circulation 99, 1222–1229.
[10] Yuan, X.M. (1999) Free Radical Res. 30, 221–231.
[11] Li, W., Yuan, X.M. and Brunk, U.T. (1998) Free Radical Res. 29, 389–398.
[12] Magnusson, M.K., Sigvaldason, H. and Magnusson, S. (1994) Circulation 89, 102–108.
[13] Berge, L.N., Bonaa, K.H. and Nordoy, A. (1994) Arterioscler. Thromb. 14, 857–861.
[14] Kiechl, S., Egger, G., Poewe, W. and Oberhollenzer, F. (1997) Circulation 96, 3300–3307.
[15] Stampfer, M.J., Grodstein, F., Rosenberg, I. and Willett, W. (1993) Circulation 87, 688.
[16] Liao, Y., Cooper, R.S. and McGee, D.L. (1994) Am. J. Epidemiol. 139, 704–712.
[17] Danesh, J. and Appleby, P. (1999) Circulation 99, 852–854.
[18] Dabbagh, A.J., Mannion, T., Lynch, S.M. and Frei, B. (1994) Biochem. J. 300, 799–803.
[19] Araujo, J.A., Romano, E.L., Brito, B.E., Parthe, V., Romano, M., Bracho, M., Montano, R.F. and Cardier, J. (1995) Arterioscler. Thromb. Vasc. Biol. 15, 1172–1180.
[20] Dabbagh, A.J., Shwaery, G.T., Keaney Jr., J.F. and Frei, B. (1997) Arterioscler. Thromb. Vasc. Biol. 17, 2638–2645.
[21] Salonen, J.T., Korpela, H., Nyyssonen, K., Porkkala, E., Tuomainen, T.-P., Belcher, J.D., Jacobs Jr., D.R. and Salonen, R. (1995) J. Intern. Med. 237, 161–168.
[22] Berger, T.M., Polidori, M.C., Dabbagh, A., Evans, P.J., Halliwell, B., Morrow, J.D., Roberts 2nd, L.J. and Frei, B. (1997) J. Biol. Chem. 272, 15656–15660.
[23] Ledue, T.B., Craig, W.Y., Ritchie, R.F. and Haddow, J.E. (1994) Clin. Chem. 40, 1345–1346.
[24] Finch, C.A., Cook, J.D., Labbe, R.F. and Culala, M. (1977) Blood 50, 441–447.
[25] Watt, F., Orlic, I., Loh, K.K., Sow, C.H., Thong, P., Liew, S.C., Osipowicz, O., Choo, T.F. and Tang, S.M. (1994) Nucl. Instr. Methods B85, 708–715.
[26] Watt, F. (1995) Nucl. Instr. Methods B104, 276–284.
[27] Watt, F. and Grime, G.W. (1995) in: Chemical Analysis (Johansson, S.A.E., Campbell, J.L. and Malmqvist, K.G., Eds.), Vol. 133, pp. 101–165, John Wiley and Son, Chichester.
[28] Ross, R. (1993) Nature 362, 801–809.
[29] Jacob, H.S. (1994) J. Lab. Clin. Med. 123, 808–816.
[30] Thong, P.S.P., He, Y., Lee, T. and Watt, F. (1997) Nucl. Instr. Methods B130, 460–465.
[31] Lynch, S.M. and Frei, B. (1995) J. Biol. Chem. 270, 5158–5163.